NON-UNIFORM FLOWS THROUGH A 8x34 PWR-TYPE ROD BUNDLE: PIV AND PRESSURE DROP MEASUREMENTS

Clément MELIN[1], Benjamin CARITEAU[1] and Philippe FILLION[1]

Université Paris-Saclay, CEA, Service de Thermohydraulique et de Mécanique des Fluides
91191, Gif-sur-Yvette, France

(E-mail: clement.melin@cea.fr, benjamin.cariteau@cea.fr, philippe.fillion@cea.fr)

ABSTRACT

We present the METERO-V experimental facility, which is a closed water loop, equipped with a test section made of two halves of PWR-type rod bundles (8x34 rods and four grids) at full scale. The aim of the experimental facility is to implement independent injection of different flow rates, void fraction and temperatures at the inlet of each half rod bundle. METERO-V experimental program focuses on IBLOCA (Intermediate Break Loss of Coolant Accident), SBLOCA (Small Break) and SLB (Steam Line Break) situations where significant density effects may occur in the core, with the aim to develop models for system-scale codes and to validate them in a separated-effect way for CFD to system thermal-hydraulic scales. We present the first results for an unbalanced flow rate distribution at the inlet of the test section, varying the Reynolds number from laminar regime to fully turbulent regime. We measure pressure difference in the radial direction of the flow at different heights and relate it to velocity measurements performed thanks to PIV. The PIV measurements are also performed at different heights, either in the bare rod region or in the wake of mixing grids. Reproducibility and accuracy of the measurements is very good. Future work will consist in non-symmetrical injections of temperatures and void fraction.

KEYWORDS:
Rod bundle, PIV, pressure drop, mixing grid, cross-flow

1. INTRODUCTION

The flow is primarily vertical upwards during the reflooding phase of a Large Break LOCA or during the core uncovering of a Small Break or Intermediate Break LOCA, but there are radial transfers in the dry zone that may have a substantial impact on the cooling capacity and the Peak Clad Temperatures (PCT). Crossflows may occur in the core during a low flow rate Steam Line Break (SLB) due to the radial liquid temperature at the core's input and the highly variable power radial distribution. To accurately forecast these occurrences, one must therefore have a thorough understanding of the 3D velocity field and the pressure drops inside the core. Correlations that are not well suited to these circumstances may be used in component scale or system scale codes. This is the situation with the CATHARE code, where there is a need to improve the correlations between pressure drops in both the axial and transverse directions. When it comes to Reynolds number, flow inclination, and the pitch-to-diameter ratio of the rod-bundle encountered in a PWR core in the researched settings, correlations and experimental data appear to be lacking in the literature [1].

In order to feed in data models at component scale or system scale where 3D effects occur in the core for the aforementioned scenarios, METERO-V (V for vertical) program has been launched in the frame of the NEPTUNE project, supported by CEA, EDF, Framatome and IRSN. Data of METERO-V may also be used for CFD codes. This paper is dedicated to describe the loop and its test section. Results of the campaign dedicated to mixing and non-mixing grids pressure drops measurements and PIV measurements are also given.

2. FACILITY DESCRIPTION

METERO-V is a 20 m^3 water loop. The fluid used is softened water at ambient temperature. The temperature range is from 10 °C to 50 °C. The maximum pressure is 2.7 bar in the test section and the pH remains neutral throughout the experiments. The test section of METERO-V is composed of two unheated halves rod bundles. The experimental facility is designed to impose the boundary conditions in terms of flow rate and temperature for each half rod bundle. The pump can deliver a flow rate up to 600 m^3/h. This corresponds to a Reynolds number of 72 000 at 20 °C and more than 120 000 at 45°C. On the contrary, laminar flows with a Reynolds number down to 720 can be obtained with a stabilized flow rate of 6 m^3/h at 20°C. A flow rate dissymmetry can be created between the two half rod bundles. Furthermore, METERO-V is also designed to perform temperature dissymmetries. The mean temperature of the fluid, before any dissymmetry process, is controlled thanks to the 110 kW heat exchanger, and by the 20 kW heater in the tank. Then, the warm leg leads to a half rod bundle and the other leg leads to the second half rod bundle. The warm leg offers an 80 kW heating power input, and the cold leg is composed of a heat exchanger that dissipates up to 80 kW of energy. In terms of temperature, depending on the flow rate, the experimental facility can create a temperature dissymmetry up to 40 °C between the two rod bundles. Another specification that METERO-V offers is its capability to generate in the test section a two-phase flow. Indeed, air injection is possible at the bottom of the test section. All of the elements presented before are displayed on the schematic view of the METERO-V thermalhydraulic loop (Figure 1).

2.1. Instrumentation of METERO-V

The physical data and boundary conditions of the tests are measured using a variety of devices. The fluid's temperature and flow rate serve as boundary conditions for the tests. Four temperature sensors are positioned beneath the test portion to measure the temperature. The temperature sensors utilised are OPTITEMP TRA-P10 and PT100 probes. Regarding the temperature they measure, their uncertainty is ±0.1%. Coriolis and electromagnetic flowmeters are used to measure flow rates. Three flowmeters are arranged in parallel branches on the main leg, and the best flowmeter is selected based on the test's flow rate. With an error of 0.5% of the observed flowrate, a Krohne IFS4000 is utilised for flowrates between 20 and 150 m^3/h. A Yokogawa RFX250G is employed with an error of 1.3% of the observed rate at flowrates between 150 and 600 m^3/h. A Yokogawa RCCT38 with an error of 0.5% of the observed rate is utilised for flowrates less than 20 m^3/h. Electromagnetic flowmeters also measure the flow rate from the warm leg. As on the main leg, three Yokogawa RFX50G, RFX100G, and RFX250G flowmeters are installed in parallel. The measurement error of these flowmeters is 0.5% of the observed flow rate. The difference between the main leg's and the warm leg's flow rates is used to calculate the flow rate of the cold leg. Rosemount 2051CD and Rosemount 3051CD differential pressure transmitters are used to measure the pressure losses reported in this article. The measurement scales used by these sensors vary. METERO-V uses three different values: ±620 mbar, ±62.2 mbar, and ±7.3 mbar. The ±620 mbar, ±62.2 mbar, and ±7.3 mbar sensors have uncertainties of 250 Pa, 25 Pa, and 2,9 Pa, or 0.2% of the entire measurement range. Velocity measurements are

carried out using the PIV (Particle Image Velocimetry) method [1]. The measurement system consists of a high-power pulsed laser, a laser-synchronised PIV camera and fluid seeding. The laser is a Quantel Ultra CFR Twins 2x200 mJ laser. The laser consists of two cavities capable of sending laser pulses spaced a few µs apart at a wavelength of 532 nm. The laser is synchronised with a PIV camera that opens when the laser pulses are emitted. The cameras are Vieworks VA-16-MC cameras with a resolution of 16 million pixels. The fluid is seeded with glass beads with diameters ranging from 9 to 13 µm and a density of 1.1 g/mL. The density of these particles is very close to that of water, so their behaviour is non-intrusive to the flow. The concentration of particles in the fluid is of the order of $75\ g/m^3$.

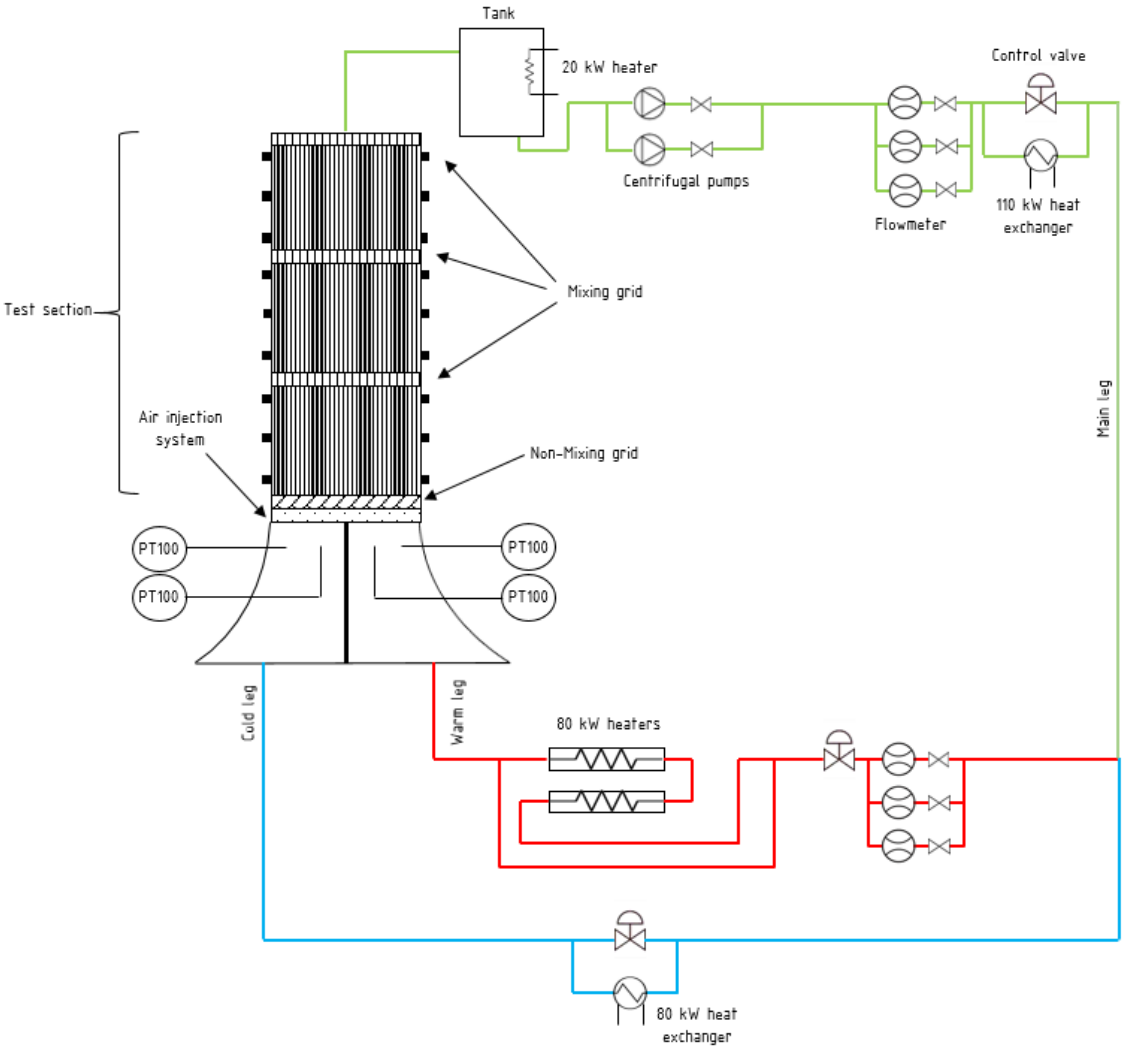

Figure 1 : Schematic view of the METERO-V thermalhydraulic loop

2.2. Geometry of the test section

The test section is rectangular with a dimension of 435x106x1789 mm. The test section is made of two unheated halves rod bundles composed of 8x37 rods, three mixing grids used in French PWR and one non-mixing grid at the inlet of the test section. The rods have a diameter of 9.5 mm and a pitch of 12.6 mm as in French PWR. The pitch P_1 between the two halves rod bundles may be changed depending on the wished distance between two PWR assemblies. These geometrical parameters are listed on the Figure 2.

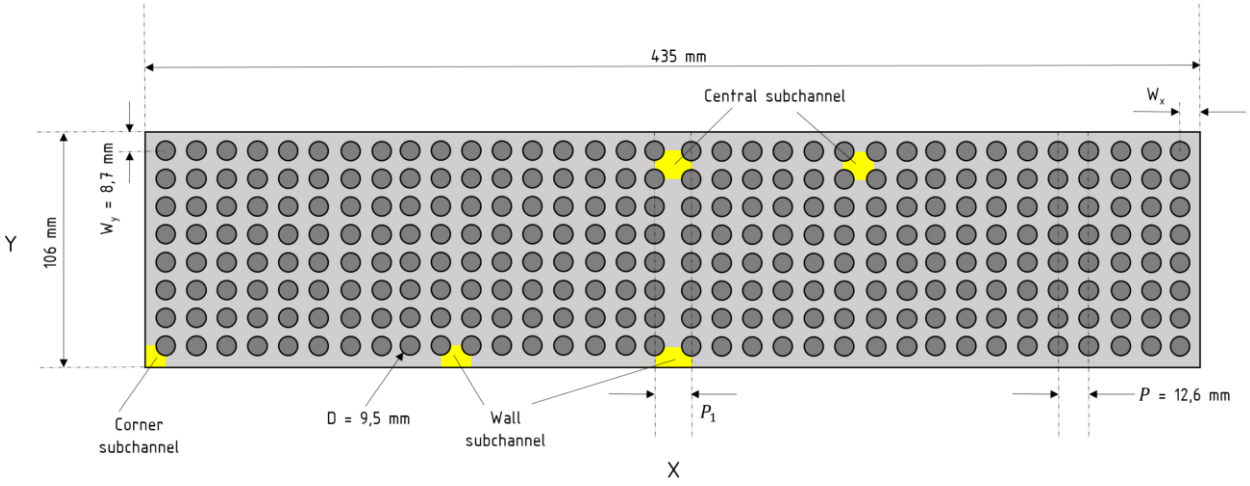

Figure 2 : Cross-section of the METERO-V test section

Nine pressure taps are available on each small side of the test section. Their localization allows the measurement of grid pressure drop and bare rod bundle pressure drop. Windows of visualization are also present to perform optical measurements.

3. RESULTS

3.1 Uncertainties of measurement

Measurements are made on METERO-V either to control the boundary conditions or to measure pressure losses. The section 2.1 lists the uncertainties related to the instruments. The pressure loss and boundary conditions measurements are used to calculate the grid friction factor. The coefficient is defined as [3]:

$$K_{grid} = \frac{\Delta P}{\frac{1}{2}\rho v^2} \tag{1}$$

The uncertainty on this coefficient is then:

$$\delta K = K\sqrt{\left(\frac{\delta \Delta P}{\Delta P}\right)^2 + \left(2\frac{\delta v}{v}\right)^2} \tag{2}$$

With ΔP the differential pressure measured, ρ the density of the fluid, v the velocity of the fluid in the bare rod region. The contribution of density is assumed to be negligible. The uncertainty on the hydraulic diameter is negligible due to the large number of rods in the test section. The uncertainty on the pressure drop measurement is defined in the section 2.1. The velocity of the fluid is deduced

from the flow rate measurement and the cross-section of the test section. The uncertainty on the velocity is then:

$$\delta v = v\sqrt{\left(\frac{\delta Q}{Q}\right)^2 + \left(\frac{\delta A}{A}\right)^2} \quad (3)$$

Due to the manufacturing tolerances: $A = (26.95 \pm 0.15) \times 10^3 mm^2$. The uncertainty on the flow rate measurement is detailed in section 2.1.

Velocity measurement using the PIV method also generates uncertainties. To quantify these, we use the method developed by Gomit et al [4]. This takes into account systematic uncertainties and the uncertainty associated with calculating velocity vectors. The uncertainty associated with the calculation of velocity vectors is calculated directly using the Davis 10.2 data processing software and is based on the Wieneke method [5]. The influencing parameters for calculating the systematic uncertainty are listed in Table 1. These parameters depend on the image calibration, the particles chosen and the uncertainty in the inter-frame time. The sensitivity coefficients C_i are then calculated in accordance with [4]. The sensitivity coefficients depend on the displacement of the particles and the time interval between the two PIV images. The C_i coefficients in the table were calculated for Re=48,000 with an average particle displacement of 6 pixels.

Table 1 : Influence parameters for calculating systematic uncertainty

Physical quantity	x_i Value	Uncertainty	$u(x_i)$	$C_i . u(x_i)$
L_{target} Length read on the calibration target	50 mm	0.5 µm	$\frac{Uncertainty}{2\sqrt{3}} = 0.14\ \mu m$	$8.16 \times 10^{-6}\ m/s$
D_{target} Number of pixels corresponding to the distance	2060 pixels	± 2 pixels reading	2 pixels	$2.83 \times 10^{-3} m/s$
$d_{particules}$ Particles influence on the surrounding flow	Diameter of 11 µm Density of 1.1 kg/m^3	Intrusiveness of the particles	$v_{max} = \frac{{d_p}^2(\rho_p - \rho_f)}{18\mu} g$ with v_{max} the Stokes velocity d_p mean diameter of the particles ρ_p density of the particles ρ_f density of the surrounding fluid μ viscosity of the surrounding fluid g the gravity	$8.84 \times 10^{-7} m/s$
Δt Time between two PIV frames	50 µs	0.05 µs	$\frac{Uncertainty}{2\sqrt{3}} = 1.44 \times 10^{-8}\ s$	$8.41 \times 10^{-4} m/s$

The systematic uncertainty is defined as :

$$u_s{}^2 = \sum_i^n C_i{}^2 \times u(x_i)^2$$

The uncertainty in the calculation of velocity vectors varies according to the quality of the measurement, i.e. homogeneous lighting, quality of seeding, particle displacement, particle size, etc. This value is given by LaVision's Davis 10.2 software and is named u_p.
The overall uncertainty u_g is then:

$$u_g = \sqrt{u_s^2 + {u_p}^2}$$

3.2 Pressure drop of mixing and non-mixing grids

The friction factor around mixing and non-mixing grids has been measured. The main difference between these grids is that mixing vanes are not present on the non-mixing grids. Due to the confidentiality of the geometry of the grids, the friction factors are not displayed on the Figure 3.

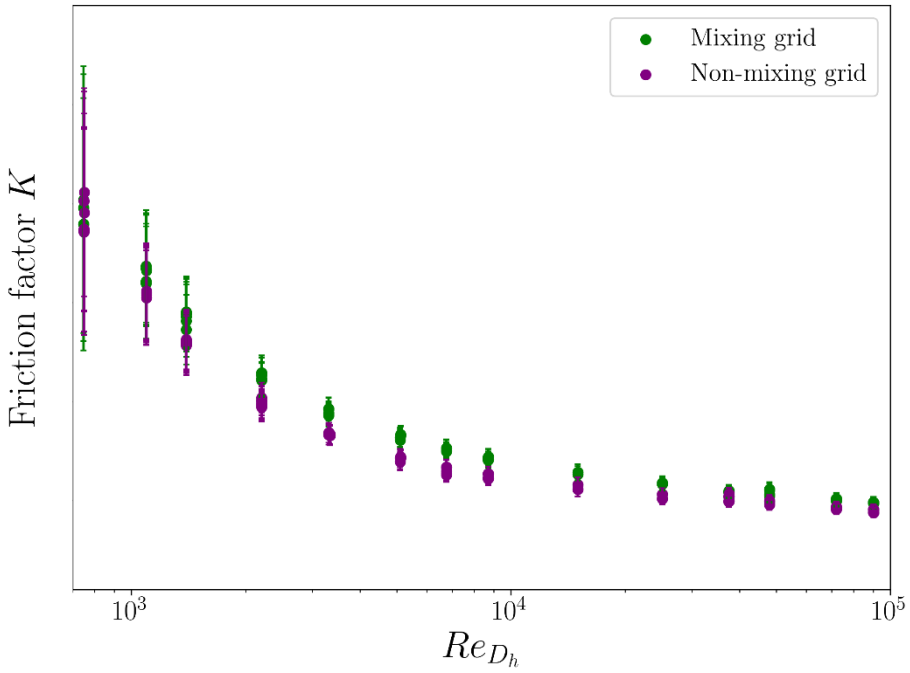

Figure 3 : Evolution of the friction factor against the Reynolds number

The friction factor decay is relevant according to some articles in the literature [3]. The friction factor have been measured for a wide range of Reynolds numbers from $Re = 750$ to $Re = 90\,000$. The effect of the mixing vanes is to increase the pressure drop of the grids. This trend is visible on the Figure 3 for each Reynolds number. The uncertainty increases as the Reynolds number decreases. The measured pressure drops are close to the uncertainty of the differential pressure transmitters for the lowest Reynolds numbers.

3.3 PIV measurements in the wake of the non-mixing-grids

As the flow is mainly vertical, the largest dissymetries of flow rates are measurable at this position. The measurements were carried out in the wake of the half non-mixing grids (Figure 1). The following parameters were used to calculate the vectors:

- Background suppression
- Selection of areas of interest (exclusion of areas masked by rods)
- Calculation of velocity vectors :

- Iterative approach used, with an initial calculation using 48x48 pixel interrogation windows, followed by 3 iterations with 32x32 pixel windows and 50% overlap. This results in a vector field resolution of 16x16 pixels, giving a physical resolution of 390µmx390µm.
- "Strongly Remove and Iteratively Replace" [6] post-processing filter to remove outliers

Measurements in the wake of the half non-mixing grids are shown in Figure 4 and in Figure 5. As with the preliminary tests, the velocities are time-averaged over 1000 images and adimensioned by the flow velocity. For these measurements, the Reynolds number was set at 48,000. Several inlet flow configurations were tested, ranging from the symmetrical case (50:50) to the extremely asymmetrical case, i.e. 90% of the flow on the left branch and 10% of the flow on the right branch (90:10). Although the differences in flow rates are very large, the velocity fields are relatively homogeneous whatever the flow rate asymmetries implemented. The central sub-channel shows a much lower velocity than the neighbouring sub-channels. This slowing of the flow may be due to the wake of the separator plate. Another hypothesis is that the space between the two half-grids is very small and therefore slows the flow considerably.

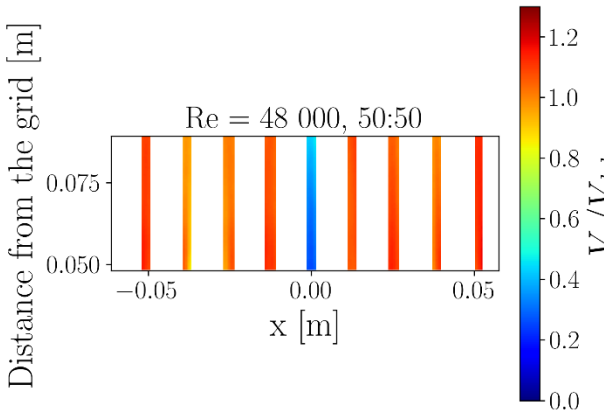

Figure 4 : Axial velocity field at the inlet of the test section for symmetrical boundary conditions

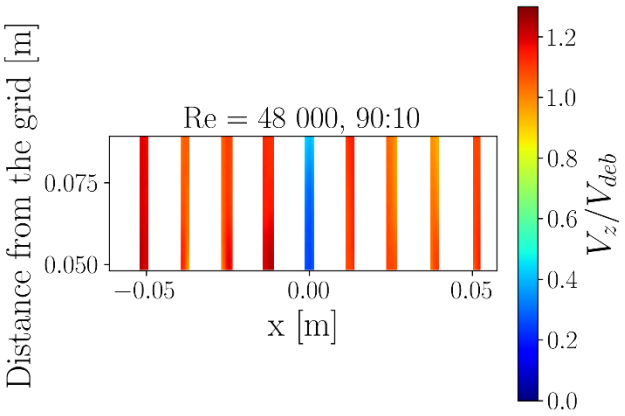

Figure 5: Axial velocity field at the inlet of the test section for asymmetrical boundary conditions

Figure 5 shows the velocity profiles at 0.058 m from the median plane of the half-grids to give a better idea of the variations in velocity as a function of the asymmetries. When the flow rate increases in the left branch, the velocity values increase in the sub-channels. Similarly, when the flow rate decreases in the right-hand branch, velocities are slightly reduced. However, the deviations measured with the PIV are negligible compared with the deviations imposed at the input. In addition, Figure 6Figure 5 shows two repeatability tests for each configuration. The tests are repeatable and overlap perfectly.

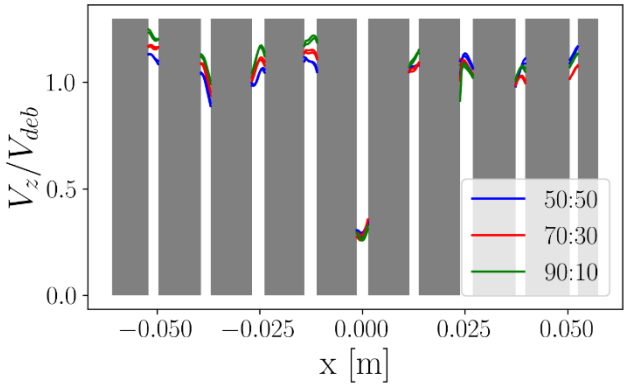

Figure 6 : Velocity profiles 0.058 m above the non-mixing grid at the inlet of the test section

Moreover, the uncertainty of these measurements has been calculated for each velocity field displayed. The maximum uncertainty found for each vector field is equal to 1.3% of the average velocity. The measured homogenization of the flow rate might be explained by the presence of the non-mixing grid just below these measurements. There is also a slight gap of around 80 mm between the end of the separator plate that keeps the flow dissymmetrical and the rod bundle.

4. CONCLUSIONS

In this study, the mixing and non-mixing grids friction factors have been studied in an 8x34 rod bundle. The evolution of the friction factor against the Reynolds number is in good agreement with the literature. The effect of the mixing vanes is visible as it increases the friction factor. The first experimental campaign with dissymmetrical flowrates at the inlet of the test section has been performed. The results were not as expected as the dissymmetrical behavior is quite flatten by the non-mixing grids and the gap between the separator plate and the rod bundle. Further geometrical modifications on the test section are needed to prevent the homogenization of the flow at the inlet of the test section. The PIV methodology is adapted to METERO-V from the implementation to the uncertainty quantification. The measurements leads to high quality data with very low uncertainty and high resolution. Further tests with dissymmetrical boundary conditions in terms of temperature and void fraction are to be performed.

5. ACKNOWLEDGEMENTS

METERO-V program is achieved in the framework of the NEPTUNE project, financially supported by CEA, EDF, Framatome and IRSN.

6. REFERENCES

[1] Bestion D., Fillion P., Préa R. and Bernard-Michel G., “Improved PWR LOCA Simulations Through Refined Core 3D Simulations – An Advanced 3D Modelling and the Associated METERO Validation Program”, Proceedings of NUTHOS-12, 2018

[2] *Particle Image Velocimetry: A Practical Guide,* Raffel, M. & Willert, Christian & Wereley, Steve & Kompenhans, Juergen, 2007

[3] Rehme K., “Pressure Drop Correlations for Fuel Element Spacers”, Nuclear Technology, 17:1, 15-23, 1973

[4] Gomit G., Beaulieu C., Braud P., David L., “Démarche d’estimation des incertitudes en PIV basée sur la méthode GUM”, 16ème Congrès Francophone de Techniques Laser pour la mécanique des fluides, 2018

[5] Wieneke B., “PIV uncertainty quantification from correlation statistics”, Measurement Science and Technology, 26(7), 074002, 2015

[6] *Flowmaster - Davis 10.2* / LaVision